An efficient phosphorus scavenging from aqueous solution using magnesiothermally modified bio-calcite

Munir Ahmad , Mahtab Ahmad , Adel R. A. Usman , Abdullah S. Al-Faraj , Yong Sik Ok , Qaiser Hussain , Adel S. Abduljabbar & Mohammad I. Al-Wabel

 View supplementary material

 Accepted author version posted online: 26 May 2017.
 Published online: 09 Jun 2017.

 Submit your article to this journal

 Article views: 11

 View related articles

 View Crossmark data

Taylor & Francis
Taylor & Francis Group

Check for updates

An efficient phosphorus scavenging from aqueous solution using magnesiothermally modified bio-calcite

Munir Ahmad[a], Mahtab Ahmad[a], Adel R. A. Usman [a,b], Abdullah S. Al-Faraj[a], Yong Sik Ok[c], Qaiser Hussain[a,d], Adel S. Abduljabbar[e] and Mohammad I. Al-Wabel [a]

[a]Soil Sciences Department, College of Food & Agricultural Sciences, King Saud University, Riyadh, Kingdom of Saudi Arabia; [b]Department of Soils and Water, Faculty of Agriculture, Assiut University, Assiut, Egypt; [c]Korea Biochar Research Center & Department of Biological Environment, Kangwon National University, Chuncheon, South Korea; [d]Department of Soil Science and Soil Water Conservation, Pir Mehr Ali shah, Arid Agriculture University, Rawalpindi, Pakistan; [e]Industrial Psychology, College of Education, King Saud University, Riyadh, Kingdom of Saudi Arabia

ABSTRACT

Bio-calcite (BC) derived from waste hen eggshell was subjected to thermal treatments (calcined bio-calcite (CBC)). The BC and CBC were further modified via magnesiothermal treatments to produce modified bio-calcite (MBC) and modified calcined bio-calcite (MCBC), respectively, and evaluated as a novel green sorbent for P removal from aqueous solutions in the batch experiments. Modified BC exhibited improved structural and chemical properties, such as porosity, surface area, thermal stability, mineralogy and functional groups, than pristine material. Langmuir and Freundlich models well described the P sorption onto both thermally and magnesiothermally sorbents, respectively, suggesting mono- and multi-layer sorption. Langmuir predicted highest P sorption capacities were in the order of: MCBC ($43.33 \, mg \, g^{-1}$) > MBC ($35.63 \, mg \, g^{-1}$) > CBC ($34.38 \, mg \, g^{-1}$) > BC ($30.68 \, mg \, g^{-1}$). The MBC and MCBC removed 100% P up to $50 \, mg \, P \, L^{-1}$, which reduced to 35.43 and 39.96%, respectively, when P concentration was increased up to $1000 \, mg \, L^{-1}$. Dynamics of P sorption was well explained by the pseudo-second-order rate equation, with the highest sorption rate of $4.32 \, mg \, g^{-1} \, min^{-1}$ for the MCBC. Hydroxylapatite [$Ca_{10}(PO_4)_6(OH)_2$] and brushite [$CaH(PO_4) \cdot 2H_2O$] were detected after P sorption onto the modified sorbents by X-ray diffraction analysis, suggesting chemisorption as the operating sorption mechanism.
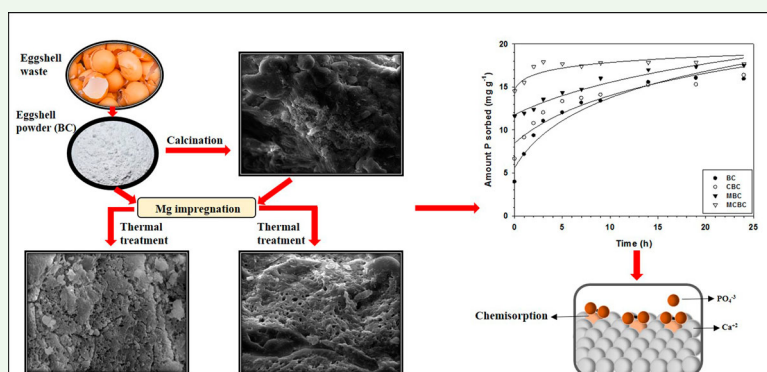
1. Introduction

Water pollution affects the health of more than one-third of the world population, causing 1.6 million deaths annually around the globe [1]. Among the chemical pollutants, phosphorus (P) is known to be the biggest cause of water quality deterioration for its creation of toxic algal blooms, dead zones and loss of biodiversity. Phosphorous is contaminating drinking water, ground water and surface water bodies worldwide. About 5.6 mega tons of P is being disposed of into rivers annually worldwide, out of which 60% is anthropogenic [2]. An average P concentration of $14.0 \, mg \, L^{-1}$ in municipal wastewater of

different countries has recently been reported, which is 14 times higher than the permissible limit of 1.0 mg L^{-1} for safe human health [3]. Excess P levels in industrial and municipal effluents result in eutrophication of surface water, by producing cyanobacterial blooms which destroys aquatic life, pollute the sources of drinking and agricultural water, ultimately affecting human health by disturbing the food chain [4,5]. To fulfill the requirements of the exponentially growing world population, usage of reclaimed water is also getting huge attention [6]. However, excessive P must be removed efficiently from these water streams prior to discharge into the environment and utilization for drinking purposes [7].

Conventional effluent treatment plants may be inadequate to remove P, and often require tertiary treatment [8]. Therefore, an innovative technique for efficient P removal is required with environment-friendly, cost-effective and less chemical additives pre-requisites. Among various techniques, sorption could be the simplest technique to remove excessive P from water. However, sorbent selection is of great importance to achieve high sorption efficiency, low cost and proper disposal of contaminant-loaded sorbent material. Consequently, alternative cheap sources of sorbent materials need to be explored.

Globally, about 1.6 billion tons of food is being wasted annually [9]. On a wet weight basis, eggshell contributes to around 4% of the total food waste [10]. Around 250,000 tons of eggshell waste is being generated annually worldwide [11]. With a consumption of 5 billion eggs in a year, Saudi Arabia is the 3rd biggest poultry products consumer in the world, generating a huge amount of eggshell waste [12]. Disposal of waste eggshells remains an environmental issue. Sustainable reuse of eggshells in a beneficial way could help in solving its disposal problem. Calcite ($CaCO_3$) is the main constituent (85–95%) of eggshell (here named as bio-calcite (BC)) that has potential to be applied as an alternative cheap sorbent for contaminants' removal from wastewater [13]. Presence of various functional groups (carbonyl, –OH, –NH$_2$, –COOH) can also make BC more effective for adsorption of various contaminants [14]. Moreover, the efficiency of BC can be enhanced by physico-chemical modifications. For example, Ahmad et al. [15] reported that thermal treatment of eggshell powder at 900℃ resulted in higher sorption efficiency for Pb than raw eggshell powder. Likewise, chemical impregnation with Fe and Mg can also enhance the sorption efficiency [16,17]. Specifically, Mg incorporated in calcite ($CaCO_3$) can cause significant changes in morphology of the calcite, which can further enhance its sorption efficiency [18]. Thermalizing the BC derived

from eggshell waste with Mg may produce a magnesiothermally reduced composite material with a potential of P removal from aqueous media. Tang et al. [19] suggested that magnesiothermal reduction of BC produces graphene-like material as a result of carbon deposition on Mg from the evolved CO_2 from eggshell powder during thermal process, according to the following equation:

$$CaCO_3 + 2Mg \rightarrow CaO + 2MgO + C$$
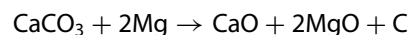
The potential of graphene as a highly efficient sorbent has recently been provoked [20]. Here, we propose that BC may be modified by magnesiothermal treatment to an efficient sorbent for P removal from water. Waste hen eggshell was used as a precursor of BC. According to our literature survey, magnesiothermally treated BC has not been previously used as adsorbent.

Hence, the present study was conducted to investigate the effectiveness of BC and its derived materials from thermal and magnesiothermal modifications for the removal of P from aqueous solution. The P sorption data were subjected to various empirical and kinetic models to predict the sorption mechanism.

2. Materials and methods

2.1. Bio-calcite preparation and modifications

Waste hen eggshells (a sustainable source of BC) were collected from the student restaurant at King Saud University Riyadh, Saudi Arabia, soaked in hot water and washed to remove impurities. The washing process was repeated four times. The washed eggshells were dried in an oven at 100℃ for 24 h, powdered in an electric grinder, sieved through 0.6 mm aperture and stored in an air tight container labeled as BC. A portion of BC powder was calcinated in an open top ceramic crucible by heating in a furnace (Carbolite, type 3216, UK) at 500℃ for 4 h. The produced calcined BC (CBC) powder was cooled down and stored in an air tight container. The BC and CBC powders were further modified by magnesiothermal reduction following the modified procedure of Tang et al. [19]. Briefly, the BC and CBC powders were mixed in 1.0 M MgCl$_2$ solution separately, using 1:1 mass/volume ratio and left to stand undisturbed for 24 h at room temperature. Materials were separated from the solution and dried in an oven at 80℃ for 24 h. The Mg-impregnated BC and CBC powders were thermalized in closed containers in a tube furnace at 700℃ for 3 h at the heating rate of 5℃ min^{-1}. The obtained materials were termed as magnesiothermalized BC (MBC) and magnesiothermalized CBC (modified calcined bio-calcite (MCBC)), respectively.

2.2. Materials' characterization

The produced materials (BC, CBC, MBC and MCBC) were comprehensively characterized for various compositional parameters. The mineralogy/crystallinity of the materials was analyzed using an X-ray diffractometer (MAXima_X XRD-7000, Shimadzu, Japan) with 30 mA Cu Kα radiation at the scan speed of 2 degree min^{-1} in continuous scan mode. The surface morphology of the materials was examined by scanning electron microscopy (SEM; EFI S50 Inspect, the Netherlands) by mounting on double-coated adhesive carbon conductive tabs (12 mm; PELCO, UK) and placed on the aluminum stubs. Different shots were captured at acceleration voltage of 30 kv and a magnification of 6000×. Thermal stability of the materials was determined by a thermogravimetric analyzer (DTG-60H, Shimadzu, Japan) recording weight loss from ambient temperature to 1100°C. Structural and functional groups were analyzed using Fourier transform infrared spectroscopy (Bruker Alpha-Eco ATR-FTIR, Bruker Optics Inc.).

2.3. Equilibrium sorption experiments

Bio-calcite (BC) and its modified derivatives (CBC, MBC and MCBC) were tested for P sorption from aqueous solution in batch-type experiments. Stock and standard P solutions in de-ionized water (18.2 MΩ cm^{-1} resistivity; Milli-Q, Germany) with different concentrations were prepared using analytical grade KH_2PO_4 (Loba Chemie, India). The materials were equilibrated with P solutions (pH adjusted at 5.5) of concentrations ranging from 1 to 1000 mg L^{-1}. Specifically, a constant weight of 10 g L^{-1} of the material was added into the P solution; and shaken in polypropylene conical tubes at 150 rpm for 24 h, after which the solutions were separated from the materials by centrifugation at 3500 rpm for 20 min, filtered through Whatman filter paper and stored at 4°C for P analysis. The molybdate-ascorbic acid method was employed for spectrophotometric determination of P in aqueous samples [21]). Three replicates of each material and a control (without material) for each specific P concentration were performed. Amount of P sorbed (q_e in mg g^{-1}) on the materials was calculated by the following Equation [22]:

$$q_e = \left[\frac{C_o - C_e}{m} \right] \times v, \tag{1}$$

where C_o and C_e are the initial and equilibrium P concentrations (in mg L^{-1}), m is the mass of material (in g) and v is the volume of the solution (in L).

Various two-parameter-based equilibrium isotherm models were applied to estimate effective sorption of the prepared materials. Non-linear forms of Freundlich, Langmuir, Temkin and Dubinin–Radushkevich equations (Equations (2–5), respectively) were exploited to fit the experimental sorption isotherms [23].

$$q_e = K_F C_e^{\frac{1}{n}}, \tag{2}$$

$$q_e = \frac{Q_L C_e K_L}{1 + K_L C_e}, \tag{3}$$

$$q_e = \frac{RT}{b} \ln (A C_e), \tag{4}$$

$$q_e = q_D \exp(- B_D [RT ln \left(1 + \frac{1}{C_e} \right)]^2), \tag{5}$$

where K_F is the Freundlich sorption capacity constant (L g^{-1}), n is the Freundlich intensity constant related to linearity, Q_L is the Langmuir maximum adsorption capacity (mg g^{-1}), K_L is the Langmuir sorption equilibrium constant (L mg^{-1}), R is the universal gas constant (8.314 J K^{-1} mol^{-1}), T is the absolute temperature, A is the binding constant (L mg^{-1}), b is the heat of adsorption, q_D is the maximum adsorption capacity of the adsorbent (mg g^{-1}) and B_D is the mean free energy of sorption used to calculate the bonding energy (E) for the ion-exchange mechanism according to Equation (6).

$$E = \frac{1}{\sqrt{2B_D}}. \tag{6}$$

Favorability of P adsorption onto the materials was assessed by using Langmuir separation factor (R_L) given by Equation (7).

$$R_L = \frac{1}{1 + K_L C_o}. \tag{7}$$

Several mathematical error functions including chi-square test (x^2), sum squares error (SSE), Marquard's percent standard deviation (MPSD), average relative error (ARE), sum of absolute error (EABS) and the coefficient of determination (R^2) were calculated to determine the closeness between the experimental adsorption data and the model-predicted data. The x^2, SSE, MPSD, ARE, EABS and R^2 were calculated by Equations (8–13), respectively [24].

$$x^2 = \sum_{i=1}^{n} \frac{(q_{ec} - q_{em})^2}{q_{em}}, \tag{8}$$

$$SSE = \sum_{i=1}^{n} (q_{ec} - q_{em})^2, \tag{9}$$

$$MPSD = 100 \sqrt{\frac{1}{n-p} \sum_{i=1}^{n} \left(\frac{q_{em} - q_{ec}}{q_{em}}\right)^2}, \quad (10)$$

$$ARE = \frac{100}{n} \sum_{i=1}^{n} \left|\frac{q_{em} - q_{ec}}{q_{em}}\right|, \quad (11)$$

$$EABS = \sum_{i=1}^{n} |q_{em} - q_{ec}|, \quad (12)$$

$$R^2 = \frac{(q_{em} - \overline{q_{ec}})^2}{\sum (q_{em} - \overline{q_{ec}})^2 + (q_{em} - q_{ec})^2}, \quad (13)$$

where q_{ec} and q_{em} are the calculated and measured amounts of P adsorbed (mg g^{-1}) onto the materials at equilibrium, n is the number of measurements and p is the number of parameters used in the model.

2.4. Kinetics sorption experiments

Batch-type kinetics sorption experiments were conducted to determine the rate of P sorption on different materials from aqueous solutions at pH 5.5. The materials were suspended in P aqueous solution (initial concentration of 200 mg L^{-1}) at the rate of 10 g L^{-1} in polypropylene conical tubes. The mixtures were shaken on a mechanical shaker at 150 rpm at room temperature. Three replicates of each material and control (without material) were performed. After 0.5, 1, 2, 3, 5, 7, 9, 14, 19 and 24 h time intervals, three tubes of each material and control were isolated. Solutions were separated from the materials by centrifugation at 3500 rpm for 20 min, filtered through Whatman filter paper, and stored at 4°C for P analysis. The equilibrium aqueous phase P concentration was determined by the molybdate-ascorbic acid method [21]. The amount of P adsorbed on per unit mass of adsorbent was calculated using Equation (1).

To predict the P sorption mechanism onto BC and its modified derivatives (CBC, MBC and MCBC), different kinetic models including first-order, second-order, pseudo-first-order, pseudo-second-order, Elovich, power function and intraparticle diffusion (Equations (14–20), respectively) were applied [25].

$$\ln q_t = \ln q_o - k_1 t, \quad (14)$$

$$\frac{1}{q_t} = \frac{1}{q_o} - k_2 t, \quad (15)$$

$$\ln (q_e - q_t) = \ln q_e - k_1' t, \quad (16)$$

$$\frac{t}{q_t} = \frac{1}{k_2' q_e^2} + \frac{1}{q_e} t, \quad (17)$$

$$q_t = \frac{1}{\beta} \ln (\alpha \beta) + \frac{1}{\beta} \ln t, \quad (18)$$

$$\ln q_t = \ln b + k_f (\ln t), \quad (19)$$

$$q_t = c + k_{id} t^{0.5}, \quad (20)$$

where q_t and q_o are the amounts of P adsorbed at time t and time 0 min, respectively (in mg g^{-1}), t is the time interval, k_1 and k_2 are the first- and second-order rate constants, respectively, q_e is the sorption capacity at equilibrium (in mg g^{-1}), k_1' and k_2' are the pseudo-first- and pseudo-second-order rate constants, respectively, α is the initial sorption rate (in mg g^{-1} min^{-1}), β is the sorption constant, b is the rate constant, k_f is the rate coefficient value (in mg g^{-1} min^{-1}), k_{id} is the apparent diffusion rate constant (in [mg g^{-1}]$^{-0.5}$) and c is the diffusion constant.

Proximity of the model-predicted coefficient values to the experimental calculated coefficient values was evaluated using various error functions (χ^2, SSE, MPSD, ARE, EABS and R^2) as given in Equations (8–13), respectively.

3. Results and discussion

3.1. Materials' characteristics

The XRD analysis indicated that calcite (CaCO$_3$) was the main constituent of BC and CBC (Figure 1(a)). However, magnesiothermal treatment resulted in the addition of Mg(OH)$_2$ and MgO in MBC and MCBC (Figure 1(b)). Previous studies have reported that eggshell powder is mainly (>90%) composed of calcite [24]. No mineralogical phase changes were observed on thermal treatment of BC. This is due to thermal stability of calcite at the selected temperature of 700°C. Calcination occurs at a temperature of ~850°C causing decomposition of CaCO$_3$ to CaO. Hence, no CaO peak was observed in any of the material. FTIR spectra further confirmed the presence of inorganic calcite in all materials (Figure 2). Main absorption bands observed at 1417, 871 and 711 cm^{-1} corresponded to calcite [26]. After magnesiothermal treatment, changes in FTIR spectra were observed. Additional bands at 3450 and 1630 cm^{-1} corresponded to hydroxyl (–OH) stretches of H-bounding due to the presence of water molecules and Mg(OH)$_2$ in MBC and MCBC [27,28]. Another distinguishable band at 675 cm^{-1} in MCBC and MBC was ascribed to Mg–O vibration [29]. Mineralogical and functional groups analyses confirmed the modification of BC and CBC as a consequence of magnesiothermal treatment. Mg in the form of MgO and Mg(OH)$_2$ was composited with CaCO$_3$ in the MBC and MCBC. However, no graphene was observed by XRD or FTIR analysis. Tang et al. [19] explained that during thermal treatment of bio-waste in the presence of Mg, the evolved CO$_2$ is
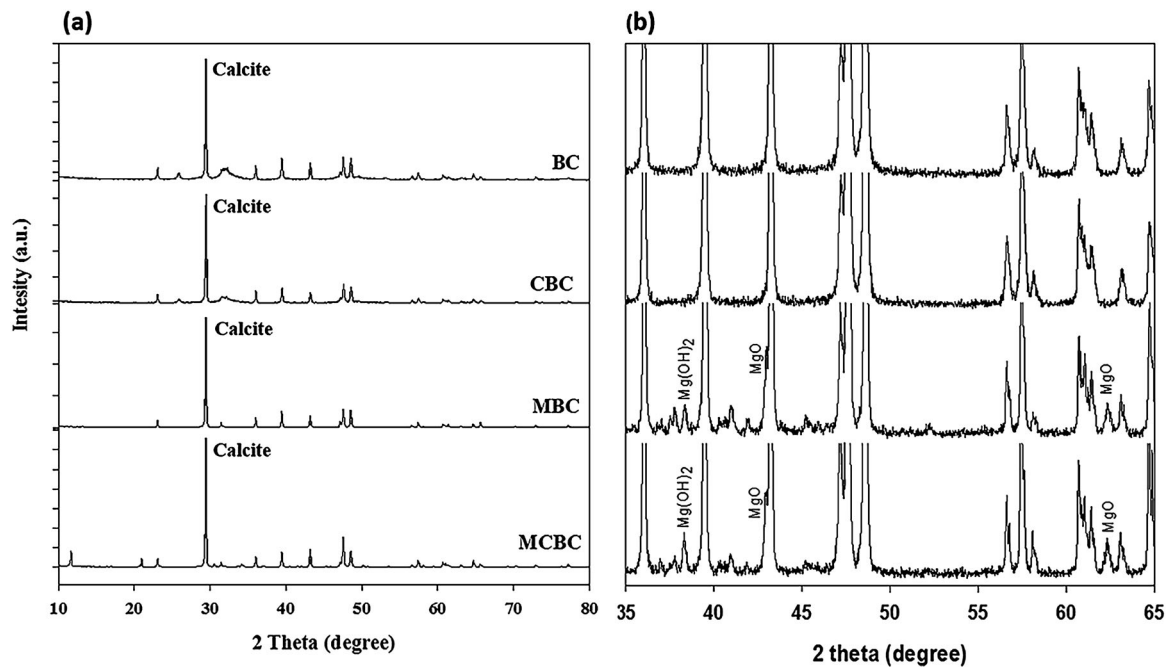
Figure 1. (a) X-ray diffraction pattern of BC, calcined bio-calcite (CBC), magnesiothermally modified bio-calcite (MBC) and magnesiothermally modified calcined bio-calcite (MCBC). (b) Magnified patterns between 35 $2\theta°$ and 65 $2\theta°$.

absorbed by MgO, resulting in graphene material. No identification of graphene could be attributed to low Mg mass (0.024 g Mg g^{-1} of eggshell) used in this study compared to the 1 g Mg g^{-1} of eggshell used by Tang et al. [19].
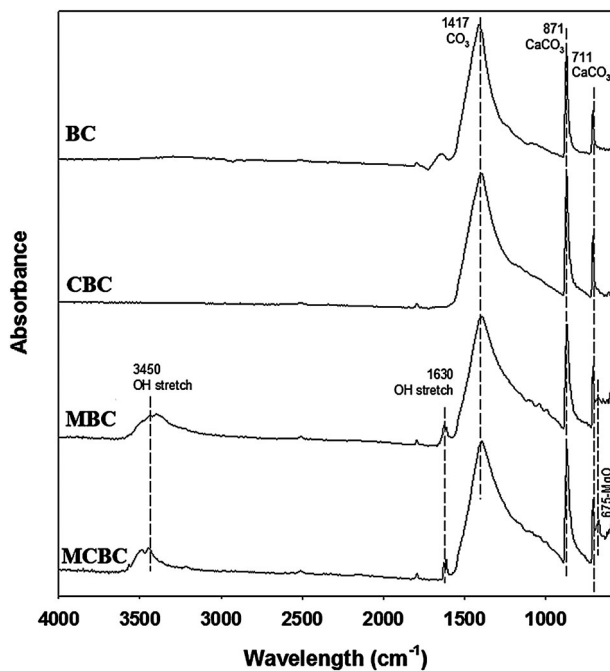

Figure 2. FTIR spectra of bio-calcite (BC), calcined bio-calcite (CBC), magnesiothermally modified bio-calcite (MBC) and magnesiothermally modified calcined bio-calcite (MCBC).

SEM images showed that thermal and magnesiothermal treatments of BC has induced changes to the surfaces of CBC, MBC and MCBC (Figure 3). The considerably crystalline surface of BC converted to porous and rough with thermal and magnesiothermal modifications, which was attributed to the loss of volatile material present in BC [30]. Thermograms showing transitional changes in the weight loss of various materials by the thermo-gravimetric analyses are shown in Figure 4. Thermal and magnesiothermal treatments resulted in decrease in weight loss of CBC (43.58%), MBC (40.91%) and MCBC (41.48%) as compared to BC (47.08%). In the BC powder, a slight weight loss at 355°C was associated to the loss of organic matter, which was not observed in other materials as a result of thermal treatment. However, small derivative peaks at <150°C in MBC and MCBC indicated water loss because of moisture absorbing ability of MgO in these materials. The main transitional change that occurred at about 740–900°C was associated to carbonate decomposition i.e. removal of CO_2 from $CaCO_3$ [30]. Similar results has already been reported by Petkova et al. [31], suggesting that decomposition of eggshell-based materials take place in temperature range of 750–850°C. The presence of Mg in MBC and MCBC resulted in a shift of temperature from 900 to 885°C for the complete decomposition of carbonaceous materials [32]. These results indicated that both thermal and magnesiothermal treatments resulted in modified characteristics of BC-derived materials, which may impact their sorption capabilities.
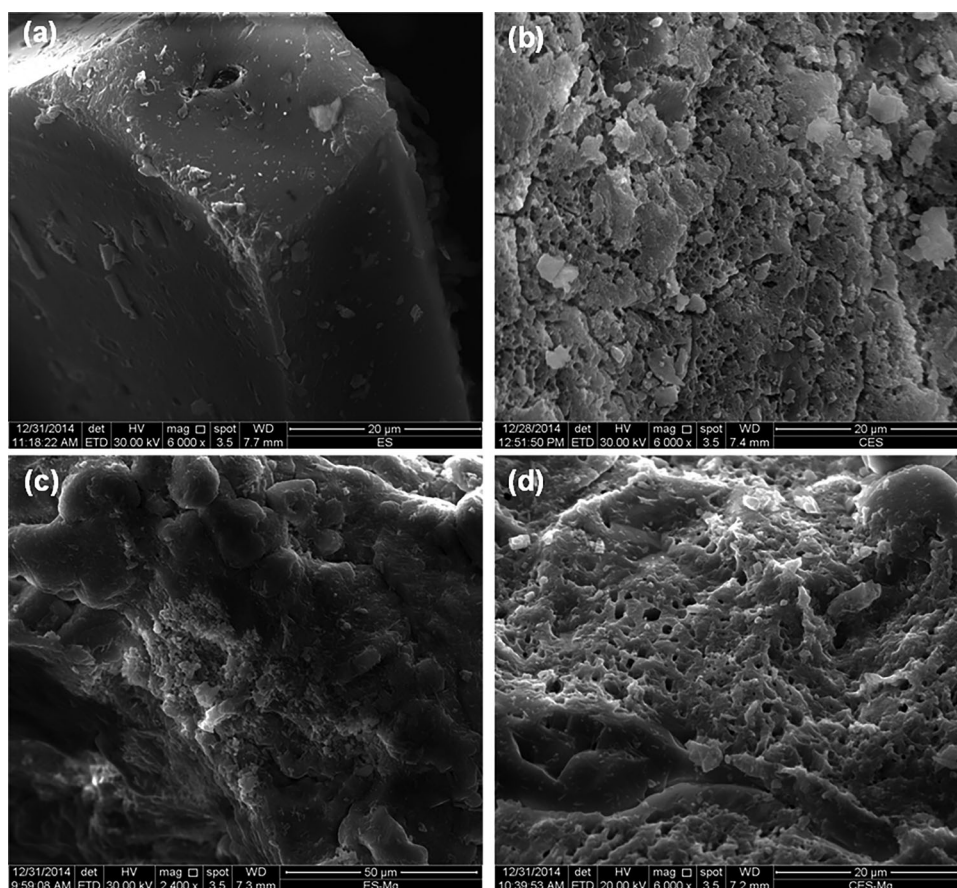
Figure 3. SEM photographs of (a) BC, (b) calcined bio-calcite (CBC), (c) magnesiothermally MBC and (d) magnesiothermally MCBC.

3.2. Equilibrium P sorption

Materials were evaluated for their efficacy toward P sorption. The sorption isotherms are shown in Figure 5. Results indicated that the amount of P sorbed (Q_e) increased with increasing initial P concentration. It has been previously reported that the type of equilibrium sorption isotherm is dependent on the initial ion concentration [13]. In this context, the sorption of P onto the various adsorbents was described by high-affinity isotherm (H-type) at low initial concentrations (up to 200 mg L^{-1}), suggesting that inner-sphere complexes (strong adsorbate-adsorptive interactions) mechanism is dominant. However, with increasing initial concentrations (above 200 mg L^{-1}), sorption isotherm was described by L-type, suggesting less availability of active sites for P

sorption. The MCBC showed a maximum P sorption (39.74 mg g^{-1}) followed by MBC (35.24 mg g^{-1}), CBC (31.55 mg g^{-1}) and BC (27.82 mg g^{-1}). The Q_e was high at low initial concentration (up to 200 mg L^{-1}) and tended to decrease at high P initial concentration (above 200 mg L^{-1}), which is ascribed to less availability of active sites for P sorption at high P concentrations. Greater P sorption onto MCBC showed its high removal efficiency than other materials.

The sorption isotherms were fitted to Freundlich, Langmuir, Temkin and Dubinin-Radushkevich models (Figure 5). The model parameters calculated from nonlinear regressions are presented in Table 1. The Freundlich model-predicted sorptive constant parameter (K_F) followed the order: MCBC (11.66 L g^{-1}) > MBC (7.21 L g^{-1}) >

Table 1. Non-linear parameters of Freundlich, Langmuir, Temkin and Dubinin–Radushkevich isotherms for P adsorption onto BC, CBC, magnesiothermally MBC and magnesiothermally MCBC.

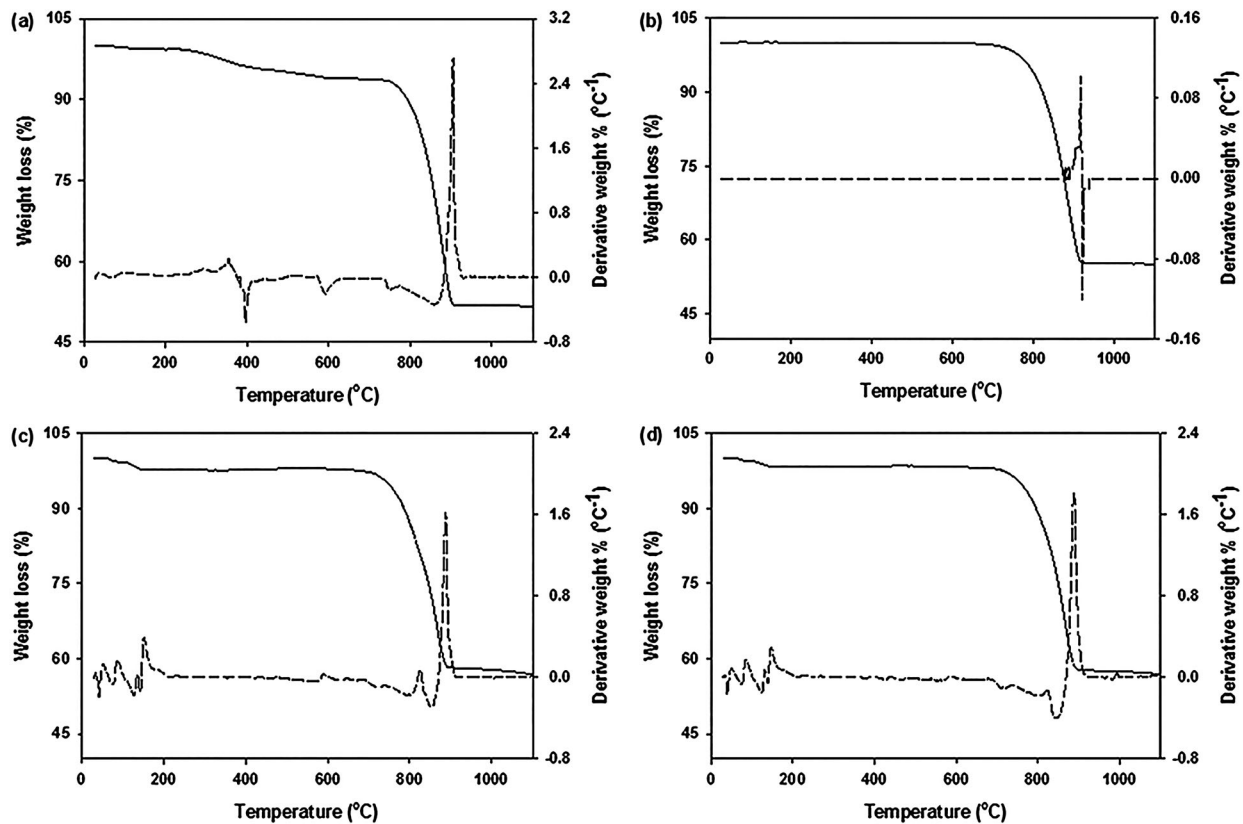| Adsorbent	Freundlich		Langmuir		Temkin		Dubinin–Radushkevich	
	K_F (mg g^{-1})	$1/n$	Q_L (mg g^{-1})	K_L (L g^{-1})	b (J mol^{-1})	A (L g^{-1})	Q_D (mg g^{-1})	E (kJ g^{-1})
BC	3.46	0.34	30.68	0.03	3.73	1.90	29.28	0.69
CBC	3.76	0.35	34.38	0.03	4.96	1.06	32.63	0.70
MBC	7.21	0.25	35.63	0.02	1.11	9.82×10^6	36.46	0.32
MCBC	11.66	0.20	43.33	0.03	1.408	1.61×10^7	37.43	1.61

Figure 4. Thermograms of (a) BC, (b) calcined bio-calcite (CBC), (c) magnesiothermally MBC and (d) magnesiothermally MCBC.

CBC (3.76 L g^{-1}) > BC (3.46 L g^{-1}), which indicated high sorption onto heterogeneous surfaces of MCBC and MBC. The 1/n values were between 0.20 and 0.35 suggesting mildly rising (favorable) isotherms for all materials [33], explaining the formation of strong bonds between P and sorbents. From the previous literature, it has been suggested that 1/n values lower than unity favor the adsorption intensity. In the current study, lower 1/n values (<1) suggested that the adsorption intensity was favorable. Maximum P sorption capacity (Q_L) predicted by the Langmuir isotherm model also followed a similar trend, i.e. MCBC (43.33 mg g^{-1}) > MBC (35.63 mg g^{-1}) > CBC (34.38 mg g^{-1}) > BC (30.68 mg g^{-1}). The Temkin model was found unsuitable to describe P sorption onto the materials. Furthermore, the Dubinin–Radushkevish model-predicted high sorption capacities (Q_D) for MCBC (37.43 mg g^{-1}) and MBC (36.46 mg g^{-1}) than CBC (32.63 mg g^{-1}) and BC (29.28 mg g^{-1}). The bonding energy (E) for all materials was $<8.0 \text{ KJ g}^{-1}$ assuming that ion-exchange could not be a favorable mechanism of P sorption [34]. All the applied models described that the materials exhibited P sorption capacity in the following order: MCBC > MBC > CBC > BC. Greater P sorption capacity of MCBC and MBC could be associated with their high reactivity resulting from thermal and magnesiothermal treatments. Specifically, the presence of MgO

and $Mg(OH)_2$ in MCBC and MBC (Figure 1) may have resulted in enhanced P sorption than other materials. Xie et al. [35] revealed that $Mg(OH)_2$ could sorb P via surface complexation forming $Mg_3(PO_4)_2$ and $MgHPO_4$.

Comparison of sorption capacity of magnesiothermally treated BC with other Mg-treated sorbents was difficult because of little information available. Recently, a few studies used Mg-treated biochar for P removal from aqueous solution. For example, Park et al. [36] activated biochar with MgO and reported maximum P sorption capacity of 8.42 mg g^{-1}, which is five times lower than in this study. On the other hand, Fang et al. [17] reported 177 mg g^{-1} P sorption capacity of Mg-modified biochar, which is four times higher than in this study. The higher P sorption capacity of Mg-biochar compared to magesiothermally treated BC is attributed to different characteristics of the materials. For instance, Mg-biochar had high surface area ($490 \text{ m}^2 \text{ g}^{-1}$), nano-Mg particles and abundance of organic functional groups, whereas magnesiothermally treated BC has very low surface area ($0.76 \text{ m}^2 \text{ g}^{-1}$), without nano particles and organic functional groups (carboxyl, hydroxyl, alcohol). Nevertheless, the sorption capacity of magesiothermally treated BC was two times higher than calcined (thermally treated at 800°C) BC (23.02 mg g^{-1}) reported by Köse and Kıvanc [37].
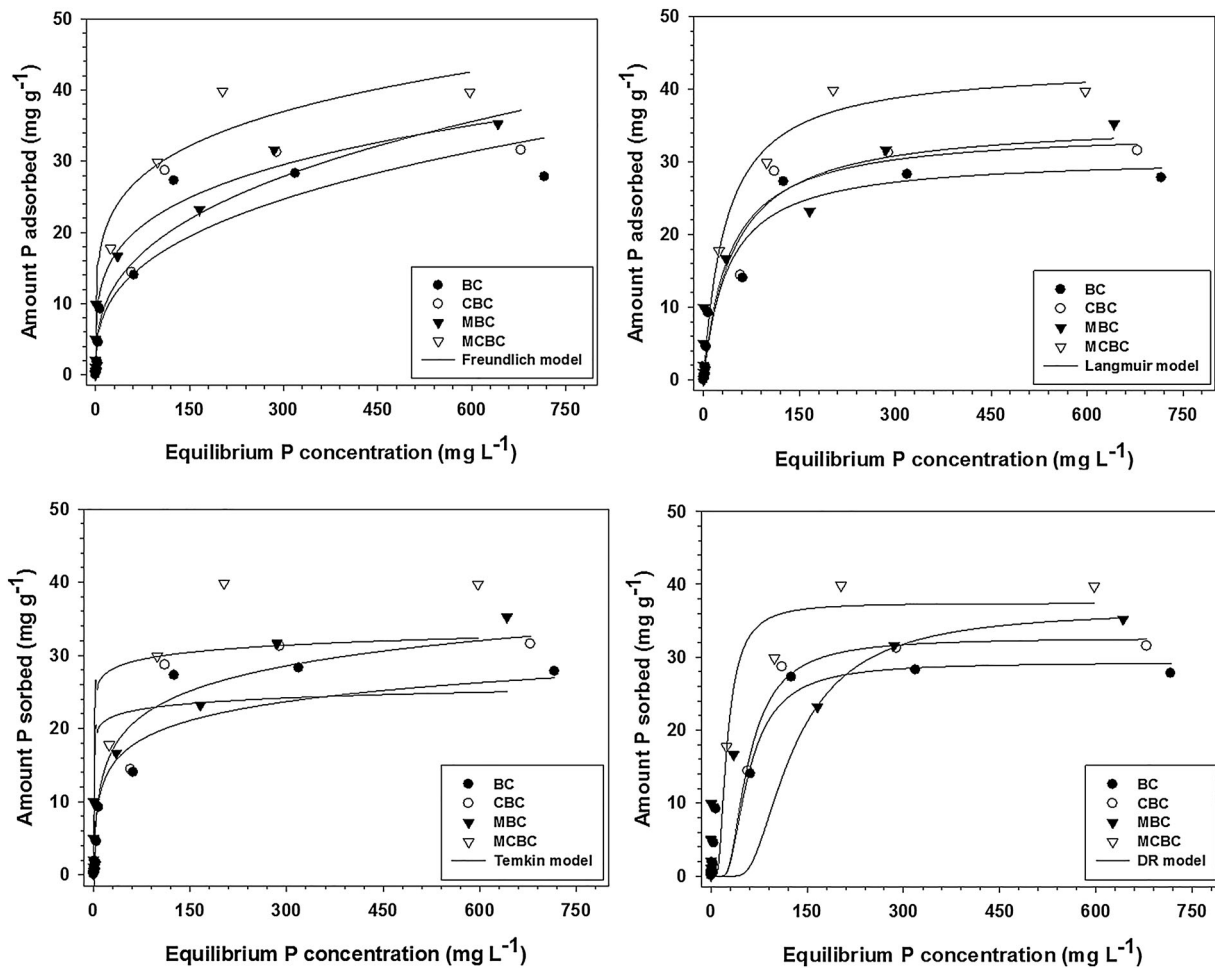
Figure 5. P sorption isotherms fitting on (a) Freundlich, (b) Langmuir, (c) Temkin and (d) Dubinin–Radushkevich (DR) models by bio-calcite (BC), calcined bio-calcite (CBC), magnesiothermally modified bio-calcite (MBC) and magnesiothermally modified calcined bio-calcite (MCBC).

Various error functions were used to depict the best model fitting the experimental P sorption data (Table S1 in supplementary materials). The results indicated that in general, the Freundlich model described well the P sorption onto MBC and MCBC, whereas Langmuir and Debunin–Radushkevich were more close to the experimental P sorption data for BC and CBC, respectively. Correlation coefficient (R^2) is the most widely accepted parameter for examining the best model fitting the experimental data. Based on the R^2 values, the Freundlich model was more applicable to magnesiothermally treated materials (MBC and MCBC) while the Langmuir model described well the P sorption onto untreated material (BC) and thermally treated material (CBC). These findings illustrated that P sorption onto MBC and MCBC was associated to their heterogeneous surfaces, whereas mono-layer sorption was predominant for BC and CBC.

Favorability of the tested materials for P sorption was assessed from an additional useful parameter of Langmuir isotherm, the separation factor (R_L) (Figure S1). The value of R_L indicates whether the isotherm is irreversible ($R_L = 0$), favorable ($0 < R_L < 1$), linear ($R_L = 1$) or unfavorable ($R_L > 1$). R_L values between 0 and 1 were obtained suggesting the present sorption system is favorable [38]. The relationship between R_L and C_0 showed that the R_L values decreased with an increase in the C_0 values (Figure S1). The values of R_L calculated in the investigated range of the initial added P concentrations are determined to be in the range of 0.037–0.097 for BC, 0.039–0.097 for CBC, 0.045–0.978 for MBC and 0.034–0.970 for MCBC. This result suggests that the investigated modified adsorbents are suitable for removal of P from aqueous solutions. These results agree with previous conclusions that the chemically modified adsorbents by Mg compounds are of importance due to creating binding sites with high affinity and adsorption efficiency in removal of anionic contaminants from aqueous solutions and water [39].
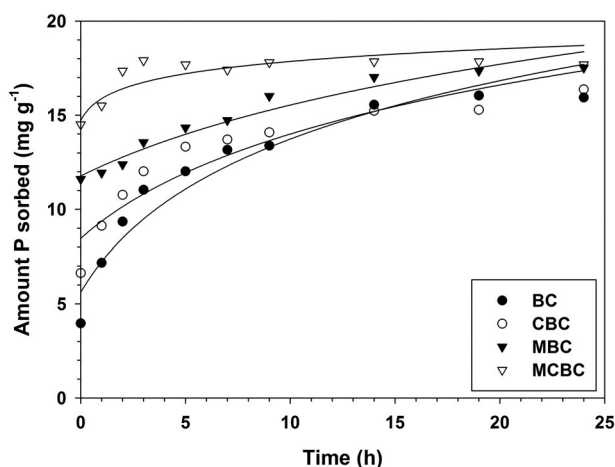
Figre 6. Adsorption kinetics of P onto bio-calcite (BC), calcined bio-calcite (CBC), magnesiothermally modified bio-calcite (MBC) and magnesiothermally modified calcined bio-calcite (MCBC).

3.3. Kinetics P sorption

Dynamics of P sorption onto different materials are shown in Figure 6. Maximum sorption was observed for MCBC within 3 h of equilibrium time resulting in 87.31% removal of P. Other materials showed longer equilibrium time. MBC, CBC and BC removed 85.41, 81.87 and 79.69% P after 24 h. Relatively rapid P sorption was achieved after 5 h followed by a slow sorption phase until equilibrium time of 24 h, which is owning to the initial high availability of sorption sites that gradually became loaded with P resulting in slow sorption. Kinetics P sorption data were subjected to various kinetic models including first-order, second-order, pseudo-first-order, pseudo-second-order, Elovich, power function and intraparticle diffusion. Parameters calculated from these kinetic models are presented in Table 2. Rate constant determines the time duration of a chemical process to complete. The higher the rate constant, shorter is the time taken to complete the reaction. In this study, high rate constants were calculated from second-order ($k_2 = 48.5 \times 10^{-5}$), pseudo-first-order ($k'_1 = 0.06 \times 10^{-1}$), pseudo-second-order ($k'_2 = 13.6 \times 10^{-3}$) and power function ($b = 2.58$) for MCBC, indicating a short time required for P sorption than other materials, which is also apparent from the

kinetics isotherms (Figure 6). Analysis of the rate constants suggested that the pseudo-second-order model described better the P sorption. The initial sorption rate (h) followed the order: MCBC (4.32 mg g^{-1} min^{-1}) > MBC (0.34 mg g^{-1} min^{-1}) > CBC (0.24 mg g^{-1} min^{-1}) > BC (0.16 mg g^{-1} min^{-1}), which agrees with the corresponding rate constants. Likewise, the Elovich model also predicted similar order of initial sorption constant (a). The sorption capacity (q_e) derived from pseudo-second-order was also higher for MBC and MCBC than CBC and BC, which is consistent with the sorption capacities predicted by Freundlich and Langmuir models (Table 1). Rate coefficient (k_f) value determined from the power function model was higher for BC (0.33 mg g^{-1} min^{-1}) followed by CBC (0.21 mg g^{-1} min^{-1}), MBC (0.12 mg g^{-1} min^{-1}) and MCBC (0.05 mg g^{-1} min^{-1}) reflecting gradual increase in P sorption with time. Intraparticle diffusion models help to understand the involvement of diffusion in the sorption mechanism [40]. In the current study, plot of P sorption against $t^{0.5}$ represents three steps of diffusion helping to understand the sorption process i.e. rapid, slow and equilibrium steps of sorption. While calculating the intraparticle diffusion parameters, only linear portion, representing the slow step, was taken into account (Table 2). Highest apparent diffusion rate constant (k_{id}) was observed for MCBC (0.45 [mg g^{-1}]$^{-0.5}$) followed by CBC (0.44 [mg g^{-1}]$^{-0.5}$), BC (0.38 [mg g^{-1}]$^{-0.5}$) and MBC (0.23 [mg g^{-1}]$^{-0.5}$); diffusion constant (c) was higher for MCBC (12.1), followed by MBC (10.26), CBC (5.87) and BC (4.19), indicating a quick sorption of P due to interparticle diffusion onto MCBC as compared to the other materials.

Examination of various error functions estimated that first-order and second-order models were not appropriate for the P sorption onto different tested materials (Table S2). Based on the R^2 values, the pseudo-second-order model best fitted the P sorption data for all materials followed by the Elovich model. Other error functions projected that in general, P sorption onto BC and CBC was well described by the Elovich model, while pseudo-second-order and intraparticle diffusion models were more applicable to P sorption onto MCBC and MBC, respectively.

Table 2. Parameters derived from the kinetic models for P sorption onto BC, CBC, magnesiothermally MBC and magnesiothermally MCBC.

Adsorbent	First-order k_1	Second-order k_2	Pseudo-first-order		Pseudo-second-order			Elovich		Power function		Intraparticle diffusion[a]	
			k'_1	q_e	k'_2	q_e	h	a	B	k_f	b	k_{id}	C
BC	0.07×10^{-2}	7.35×10^{-5}	0.04×10^{-1}	2.50	0.53×10^{-3}	17.21	0.16	0.49	0.32	0.33	0.55	0.38	4.19
CBC	0.04×10^{-2}	3.94×10^{-5}	0.03×10^{-1}	1.96	0.87×10^{-3}	16.64	0.24	1.75	0.42	0.21	1.31	0.44	5.87
MBC	0.03×10^{-2}	2.03×10^{-5}	0.04×10^{-1}	2.02	1.03×10^{-3}	18.02	0.34	29.46	0.58	0.12	1.99	0.23	10.26
MCBC	0.01×10^{-2}	48.5×10^{-5}	0.06×10^{-1}	0.85	13.6×10^{-3}	17.83	4.32	1.89×10^{7}	1.32	0.05	2.58	0.45	12.10

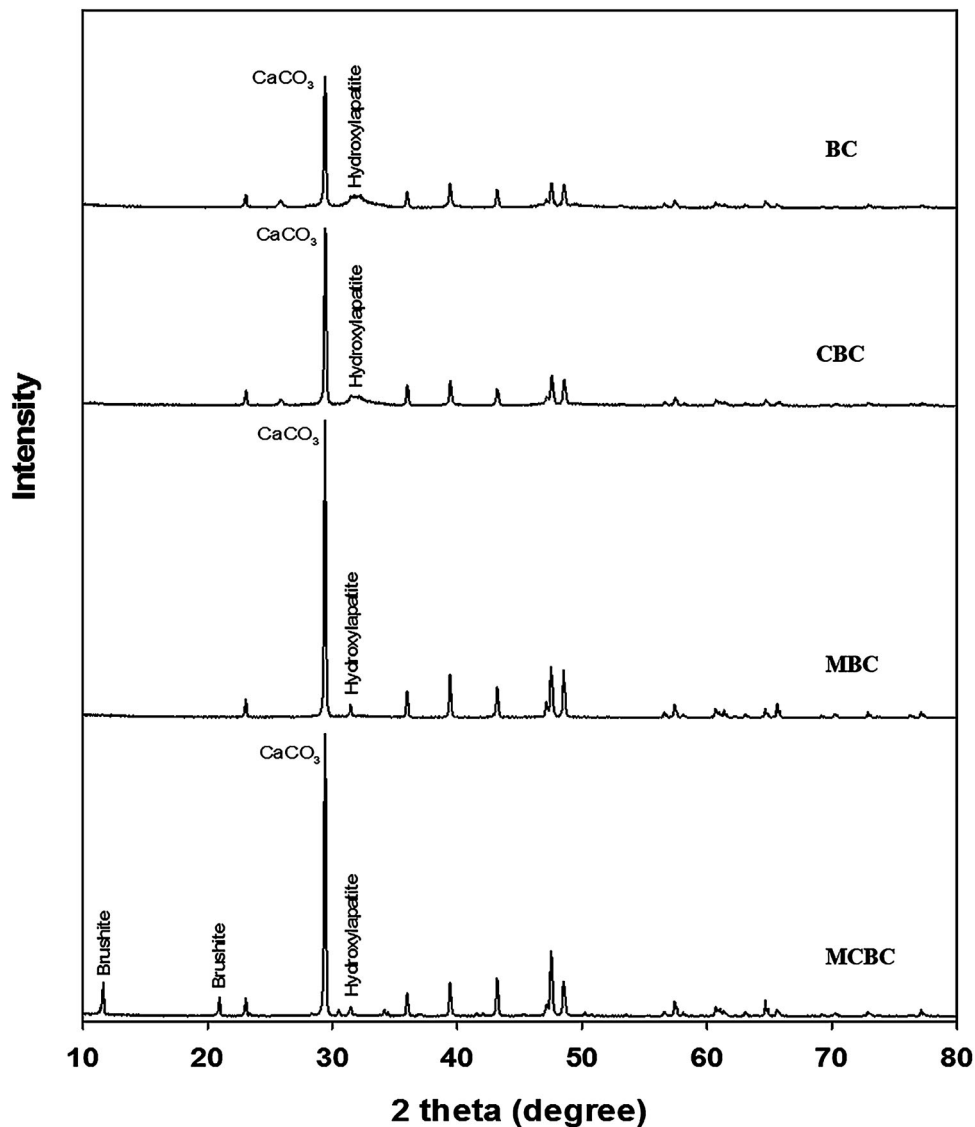[a]Parameters were calculated based on the linear portion of the data.

Figure 7. X-ray diffraction patterns of bio-calcite (BC), calcined bio-calcite (CBC), magnesiothermally modified bio-calcite (MBC) and magnesiothermally modified calcined bio-calcite (MCBC), after P sorption.

3.4. Sorption mechanism

Various empirical and kinetics equilibrium models were applied to the P sorption experimental data of different materials to evaluate the possible mechanism of P sorption. According to the closeness of experimental and modeled sorption data, the Langmuir model suggested mono-layer sorption onto homogeneous surfaces of BC, whereas porous structure of CBC (Figure 2) further facilitated the P sorption as described by the Dubinin–Radushkevich model. Heterogeneous surfaces of MBC and MCBC favored the multi-layer P sorption, based on the best fitting Freundlich model. Dynamics of P sorption clearly indicated that chemisorption (covalent binding with the functional groups) was the rate-limiting step for P sorption onto all the materials as predicted from the best fitting of experimental data to the pseudo-second-order model. This

suggested that P sorption was controlled by direct chemical interaction with sorbent surfaces. Moreover, fitting of the experimental data to the Elovich model also supported multi-layer chemisorption in which each layer exhibited different activation energy [41]. Mezenner and Bensmaili [42] reported chemisorption as an operating mechanism for P adsorption onto iron hydroxide-eggshell. In addition to chemisorption as the main operating mechanism, diffusion can be attributed to P sorption onto the sorbents as can be seen in Figure S2. It is interesting to notice that all the materials maintained the equilibrium pH between 7.30 and 7.84 even at higher initial P concentration (Figure S3), indicating the existence of HPO_4 species. Resultantly, hydroxyapatite precipitation could be possible at high initial P concentrations (>200 mg L^{-1}) [43]. Chemisorption also causes an adsorptive chemical change by

forming a surface chemical compound via covalent or ionic bonding [44]. To examine the formation of hydroxylapatite, XRD spectra of the materials after P sorption were obtained, as shown in Figure 7. Hydroxylapataite [$Ca_{10}(PO_4)_6(OH)_2$] was observed as a new mineral phase at 31.8 $2\theta°$ in all the tested materials. However, the peaks were broad in BC and CBC, and intense in MBC and MCBC. Additionally, brushite [$CaHPO_4.2H_2O$] was detected at 11.6 $2\theta°$ in MCBC after P sorption, which explained its relatively higher sorption capacity than other materials. Formation of hydroxyalapatite and brushite is expectedly favorable due to the surplus of Ca from the eggshell materials and P in the aqueous solution. Formation of hydroxylapatite and brushite are resultant chemical species of chemisorption. Therefore, it was affirmed that chemisorption was the main mechanism of P sorption onto BC and its derived CBC, MBC and MCBC materials.

4. Conclusion

Bio-calcite (BC) derived from waste hen eggshell was thermally (CBC) and magnesiothermally modified (MBC and MCBC) to produce cheap and efficient green sorbents for P removal from water. The modification imparted structural and chemical changes such as surface porosity, functional groups and mineralogical composition that further influenced the P sorption efficiency of the modified materials. At 50 mg L^{-1} P concentration in aqueous solution, magnesiothermally modified BC showed 100% P removal efficiency, suggesting that magnesiothermally modified BC was more effective in P sorption than thermally modified BC. Freundlich and Langmuir models best described the P sorption onto magnesiothermally and thermally treated materials, respectively, suggesting mono- and multi-layer chemisorption. Sorption dynamics indicated high rate constants for magnesiothermally modified BC accounting for less sorption time. The XRD analysis of thermally and magnesiothermally modified BC revealed the formation of Ca-phosphate compounds (hydroxylapataite [$Ca_{10}(PO_4)_6(OH)_2$] and brushite [$CaHPO_4.2H_2O$]) onto these sorbents as a result of chemisorption. These findings suggested that reusing of waste eggshell could (i) avoid pathogens' habitation by reducing surface pollution, (ii) efficiently remove P from industrial and domestic wastewater streams and (iii) provide a sustainable resource of P-fertilizer for acidic soils.

Disclosure statement

No potential conflict of interest was reported by the authors.

ORCID

Adel R. A. Usman http://orcid.org/0000-0001-8522-713X
Mohammad I. Al-Wabel http://orcid.org/0000-0002-6223-2953

References

[1] World Health Organization (WHO)/UN Child. Fund (UNICEF). 2008. Progress on drinking-water and sanitation: Special focus on sanitation. Geneva, (Switz.)/New York: WHO/UNICEF. p. 58.
[2] Turner RE, Rabalais NN, Justic D, et al. Global patterns of dissolved N, P and Si in large rivers. Biogeochemistry. 2003;64:297–317.
[3] Karunanithi R, Szogi AA, Bolan N, et al. Phosphorus recovery and reuse from waste streams. In: Sparks DL, editor. Advances in agronomy. Waltham: Academic Press Inc.; 2015. p. 173–250.
[4] Codd GA, Morrison LF, Metcalf JS. Cyanobacterial toxins: risk management for health protection. Toxicol Appl Pharmacol. 2005;203:264–272.
[5] Dodds WK, Bouska WW, Eitzmann JL, et al. Eutrophication of U.S. freshwaters: analysis of potential economic damages. Environ Sci Technol. 2009;43:12–19.
[6] Wang Q, Zhang B, Wang M, et al. Synthetic Lepidocrocite for phosphorous removal from reclaimed water: optimization using convex optimization method and successive adsorption in fixed bed column. Environ Technol. 2016;37(21):2750–2759.
[7] Han C, Wang Z, Yang W, et al. Investigation of the phosphorus removal capacities of basic oxygen furnace slag under variable conditions. Environ Technol. 2016;37(10):1257–1264.
[8] Rajasulochana P, Preethy V. Comparison on efficiency of various techniques in treatment of waste and sewage water – a comprehensive review. Resource-Efficient Technol. 2016;2(4):175–184.
[9] Food and Agriculture Organization (FAO). [Internet] Food wastage footprints impact on natural resources; 2009 [cited 2015 June 23]. Available from: http://fao.org/publications
[10] Qamaruz-Zaman N, Milke MW. VFA and ammonia from residential food waste as indicators of odor potential. Waste Manage. 2012;32:2426–2430.
[11] Raihana MF, Sopyan I, Hamdi M, Ramesh S. Novel chemical conversion of eggshell to hydroxyapatite powder. In: IFMBE Proceedings. 2008;21:333–336.
[12] Saudi Poultry [Internet] 2015 [cited 2015 May 15] Available from: http://www.saudipoultry.com/
[13] Ahmad M, Usman ARA, Lee SS, et al. Eggshell and coral wastes as low cost sorbents for the removal of Pb^{2+}, Cd^{2+} and Cu^{2+} from aqueous solutions. J Ind Eng Chem. 2012;18:198–204.

[14] Mafu LD, Msagati TAM, Mamba BB. Adsorption studies for the simultaneous removal of arsenic and selenium using naturally prepared adsorbent materials. Int J Environ Sci Technol. 2014;11:1723–1732.

[15] Ahmad M, Hashimoto Y, Moon DH, et al. Immobilization of lead in a Korean military shooting range soil using eggshell waste: an integrated mechanistic approach. J Hazard Mater. 2012;209-210:392–401.

[16] Usman ARA, Sallam AS, Al-Omran A, et al. Chemically modified biochar produced from Conocarpus wastes: an efficient sorbent for Fe(II) removal from acidic aqueous solutions. Adsorpt Sci Technol. 2013;31:625–640.

[17] Fang C, Zhang T, Li P, et al. Application of magnesium modified corn biochar for phosphorus removal and recovery from swine wastewater. Int J Environ Res Public Health. 2014;11:9217–9237.

[18] Kitamura M. Crystallization and transformation mechanism of calcium carbonate polymorphs and the effect of magnesium ion. J Colloid Interf Sci. 2001;236:318–327.

[19] Tang H, Gao P, Liu X, et al. Bio-derived calcite as a sustainable source for graphene as high-performance electrode material for energy storage. J Mater Chem A. 2014;2:15734–15739.

[20] Sitko R, Zawisza B, Malicka E. Graphene as a new sorbent in analytical chemistry. Trends Anal Chem. 2013;51:33–43.

[21] Murphy JA, Riley JP. A modified single solution method for the determination of phosphate in natural waters. Anal. Chim. Acta. 1962;27:31–36.

[22] Ok YS, Yang JE, Zhang YS, et al. Heavy metal adsorption by a formulated zeolite-Portland cement mixture. J Hazard Mater. 2007;147:91–96.

[23] Ahmad M, Lee SS, Rajapaksha AU, et al. Trichloroethylene adsorption by pine needle biochars produced at various pyrolysis temperatures. Bioresour Technol. 2013;143:615–622.

[24] Foo KY, Hameed BH. Insights into the modeling of adsorption isotherm systems. Chem Eng J. 2010;156:2–10.

[25] Ahmad M, Lee SS, Oh SE, et al. Modeling adsorption kinetics of trichloroethylene onto biochars derived from soybean stover and peanut shell wastes. Environ Sci Poll Res. 2013;20:8364–8373.

[26] Tsai WT, Yang JM, Lai CW, et al. Characterization and adsorption properties of eggshells and eggshell membrane. Bioresour Technol. 2006;97:488–493.

[27] Kloprogge JT, Hickey L, Frost RL. FT-Raman and FT-IR spectroscopic study of synthetic Mg/Zn/Al-hydrotalcites. J Raman Spectrosc. 2004;35:967–974.

[28] Ahmad M, Ahmad M, Usman ARA, et al. Date palm waste-derived biochar composites with silica and zeolite: synthesis, characterization and implication for carbon stability and recalcitrant potential. Environ Geochem Health. 2017;1–18. doi:10.1007/s10653-017-9947-0

[29] Tamilselvi P, Yelilarasi A, Hema M, et al. Synthesis of hierarchical structured MgO by sol-gel method. Nano Bulletin. 2013;2:130106.

[30] Lim JE, Ahmad M, Usman ARA, et al. Effects of natural and calcined poultry waste on Cd, Pb and As mobility in contaminated soil. Environ Earth Sci. 2013;69:11–20.

[31] Petkova V, Kostova B, Shopska M, et al. Behavior of high-energy-milling-activated eggshells during thermal treatment. J Thermal Anal Calorimet. 2017;1–9. doi:10.1007/s10973-016-5710-5

[32] Almerindo GI, Probst LFD, Campos CEM, et al. Magnesium oxide prepared via metal-chitosan complexation method: application as catalyst for transesterification of soybean oil and catalyst deactivation studies. J Power Sources. 2011;196:8057–8063.

[33] Tseng R, Wu F. Analyzing a liquid–solid phase countercurrent two- and three-stage adsorption process with the Freundlich equation. J Hazard Mater. 2009;162:237–248.

[34] Ho YS, Porter JF, McKay G. Equilibrium isotherm studies for the sorption of divalent metal ions onto peat: copper, nickel and lead single component systems. Water Air Soil Poll. 2002;141:1–33.

[35] Xie F, Wu F, Liu G, et al. Removal of phosphate from eutrophic lakes through adsorption by in situ formation of magnesium hydroxide from diatomite. Environ Sci Technol. 2014;48:582–590.

[36] Park JH, Ok YS, Kim SH, et al. Evaluation of phosphorus adsorption capacity of sesame straw biochar on aqueous solution: influence of activation methods and pyrolysis temperatures. Environ Geochem Health. 2015;37:969–983.

[37] Kosea TE, Kıvanc B. Adsorption of phosphate from aqueous solutions using calcined waste eggshell. Chem Eng J. 2011;178:34–39.

[38] Mohan D, Rajput S, Singh VK, et al. Modeling and evaluation of chromium remediation from water using low cost bio-char, a green adsorbent. J Hazard Mater. 2011;188:319–333.

[39] Usman ARA, Ahmad M, El-Mahrouky M, et al. Chemically modified biochar produced from Conocarpus waste increases NO₃ removal from aqueous solutions. Environ Geochem Health. 2016;38:511–521.

[40] Baláž M, Bujňáková Z, Baláž P, et al. Adsorption of cadmium(II) on waste biomaterial. J Colloid Interface sci. 2015;454:121–133.

[41] Alberti G, Amendola V, Pesavento M, et al. Beyond the synthesis of novel solid phases: review on modelling of sorption phenomena. Coordin Chem Rev. 2012;256:28–45.

[42] Mezenner NY, Bensmaili A. Kinetics and thermodynamic study of phosphate adsorption on iron hydroxide-eggshell waste. Chem Eng J. 2009;147:87–96.

[43] Hosni K, Moussa SB, Amor MB. Conditions influencing the removal of phosphate from synthetic wastewater: influence of the ionic composition. Desalination. 2007;206:279–285.

[44] Xiong W, Peng J, Hu Y. Use of X-ray absorption near edge structure (XANES) to identify physisorption and chemisorption of phosphate onto ferrihydrite-modified diatomite. J Colloid Interface Sci. 2012;368:528–532.